INTERNATIONAL JOURNAL FOR NUMERICAL AND ANALYTICAL METHODS IN GEOMECHANICS
Int. J. Numer. Anal. Meth. Geomech., **22**, 671–687 (1998)

MODELLING OF SHEARING BEHAVIOUR OF A RESIDUAL SOIL WITH RECURRENT NEURAL NETWORK

JIAN-HUA ZHU[1,*,†], MUSHARRAF M. ZAMAN[1,‡] AND SCOTT A. ANDERSON[2,§]

[1] *School of Civil Engineering and Environmental Science, The University of Oklahoma, 202 W. Boyd St., Row 334, Norman, OK 73019, U.S.A.*
[2] *Woodward-Clyde Consultants, Denver, CO* 80237, *U.S.A.*

SUMMARY

Modelling of shear behaviour of residual soils is difficult in that there is a significant variability in constituents and structures of the soil. A Recurrent Neural Network (RNN) is developed for modelling shear behaviour of the residual soil. The RNN model appears very effective in modelling complex soil shear behaviour, due to its feedback connections from an hidden layer to an input layer. Two architectures of the RNN model are designed for training different sets of experimental data which include strain-controlled undrained tests and stress-controlled drained tests performed on a residual Hawaiian volcanic soil. A dynamic gradient descent learning algorithm is used to train the network. By training only part of the experimental data the network establishes neural connections between stress and strain relations. Although the soil exhibited significant variations in terms of shearing behaviour, the RNN model displays a strong capability in capturing these variabilities. Both softening and hardening characteristics of the soil are well represented by the RNN model. Isotropic and anisotropic consolidation conditions are precisely reflected by the RNN model. In undrained tests, pore water pressure responses at various loading stages are simultaneously simulated. With a RNN model designed for a special drained test, the network is able to capture abrupt changes in axial and volumetric strains during shearing courses. These good agreements between the measured data and the modelling results demonstrate the desired capability of the RNN model in representing a soil behaviour.

Key words: recurrent neural network; residual soil; shear behaviour; simulation; prediction

INTRODUCTION

Modelling of soil behaviour plays an important role in dealing with issues related to soil mechanics and foundation engineering. Over the past three decades many researchers devoted enormous efforts collectively to model soil behaviour and proposed many mathematical models based on various assumptions.[1–3] There are generally four similar procedures followed by researchers in developing conventional constitutive models: (1) making simplified assumptions that form a basis of the model; (2) employing criteria for identifying yielding or failure state of

*Correspondence to: J.-H. Zhu, School of Civil Engineering and Environmental Science, The University of Oklahoma, 202 W. Boyd St, Room 334, Norman, OK 73019, U.S.A. E-mail: jzhu@ou.edu.
†Research Assistant.
‡Presidential Professor.
§Senior Project Engineer.

CCC 0363–9061/98/080671–17$17.50

Received 16 January 1997
Revised 30 October 1997

a soil; (3) formulating specific mathematical expressions that meet prerequisite conditions inherent in (1) and (2); (4) finding appropriate parameters used for backprediction of the soil constitutive behaviour.[2,4] The strength of the conventional model is that it has clear mechanistic concept and easily be understood by engineers. However, there are many material parameters that must be predetermined for the application of the model, and determination of these parameters requires additional laboratory experiments and optimization techniques.[1,5–7]

The application of neural network offers an alternative means for the modelling of soil behaviour.[8–10] An artificial neural network (ANN) model is fundamentally different from the conventional constitutive model. One of its distinctive features is that it is based on experimental data rather than on assumptions made in developing constitutive model, and there is no material constants needed in developing an ANN model. These features ascertain the ANN model to be an objective model that can truly represent natural neural connections among variables, rather than a subjective model which assumes variables obeying a set of predefined relations. An ANN model learns from experimental data and forms neural connection stimuli from a learning process, functioning some what like a human brain. Because of its unique learning, training and predicting characteristics, the ANN model has great potential application in soil engineering particularly for situations where good experimental data are available and where conventional constitutive modelling may be difficult and time consuming.

The available references are quite few with regard to the neural network model of soil behaviour. Ellis *et al.*[8] modelled stress–strain relation of sands using sequential and regular backpropagation neural network. It is observed that good agreement exists between laboratory data and modelling results. It is also noted that a prescribed strain rate (0·0405 per cent) has to be defined in order to make prediction with the model.[9] In this study, a Recurrent Neural Network (RNN) model is found to be more efficient than standard backpropagation network in simulating and predicting non-linear shear behaviour of a residual soil. Two different kinds of laboratory experimental data including a set of strain-controlled experiments and a set of stress-controlled experiments performed on a Hawaiian residual soil are used to train the models developed in this study. The good simulation and prediction of stress–strain behaviour in both undrained and drained tests demonstrate that the RNN approach can be effectively used to model complex soil behaviour. A fair agreement between experimental and the RNN modelled excess pore water pressure induced in undrained tests is observed. The significant variations inherent in the soil behaviour are successfully captured by using an appropriate algorithm function and architecture of the neural network.

NEURAL NETWORK PARADIGM

Neural networks have recently emerged as a very promising tool for various engineering applications. This includes pattern recognition, classification, speech recognition, manufacturing process control, and material behaviour modelling.[11–13,9] The neural network function is determined largely by connections between input and output elements. The basic one layer neural network model can be expressed as

$$\mathbf{Y} = F(\mathbf{W}^*\mathbf{X} + \mathbf{b}) \tag{1}$$

where $\mathbf{X}$ is an input vector $(X_1, X_2, \ldots, X_i, \ldots, X_n)$, $\mathbf{Y}$ is an output vector $(Y_1, Y_2, \ldots, Y_j, \ldots, Y_m)$, $\mathbf{W}$, $\mathbf{b}$ are weight matrix and bias vectors, respectively, and F is an activation function.

The major objective of the neural network is to find the connection weight **W** and bias values **b** through a training process by minimizing an appropriate error function E. To find proper weights and biases a number of epochs of training (or iteration calculation) are performed on the network. The goal of iteration is achieved when a sum of mean-squared error between target and output values is minimized or is within an acceptable range.

To facilitate efficiency of a neural network, a specific neural network architecture has to be chosen for a specific task. It is now recognized that recurrent neural networks (RNN) are usually superior to other kinds of networks in that they have both feedforward and feedbackward connections between inputs and outputs.[13–16] A typical architecture of a RNN is shown in Figure 1. The initial input **X** is propagated to the hidden layer **Z** through weights V and bias values V_0. The outcome from the hidden layer is then transmitted to the output layer **Y** through weights W and bias values W_0 and feedbackward at the same time to the input layer, working as external data inputting to the hidden layer again. The action of the RNN shown in Figure 1 can be represented by following equations:

$$Z_{jt} = F_1\left(\sum V_{ij}X_{ij} + V_0 + \sum V_{z(t-1)}Z_{i(t-1)}\right) \tag{2}$$

$$\begin{aligned} Y_{kt} &= F_2\left(\sum W_{jk}Z_{jt} + W_0\right) \\ &= F_2\left(\sum W_{jk}F_1\left(\sum V_{ij}X_{ij} + V_0 + \sum V_{z(t-1)}Z_{j(t-1)}\right) + W_0\right) \end{aligned} \tag{3}$$

where F_1 and F_2 are activation functions from the input layer to the hidden layer and from the hidden layer to the output layer, respectively; Z_{jt}, $Z_{j(t-1)}$ are outputs of node j in the hidden layer at t and $t-1$ epochs; Y_{kt} is the output of node k in the output layer at t epoch; V_{ij} refers to the weight connecting node j in the hidden layer with the node i in the input layer; $V_{z(t-1)}$ is the connection weight between outputs of the hidden layer at t epoch and $t-1$ epoch; W_{jk} is the weight connecting node k in the output layer with the node j in the hidden layer; V_0 and W_0 are biases of hidden layer and output layer, respectively.

The weight is updated by the following expression:

$$\text{Weight}_{(\text{new})} = \text{Weight}_{(\text{old})} + \text{Change of the weight}$$

The change in weight and bias can be derived by minimizing the sum of squared errors between target value T and output value Y using delta rules[17,18,11] and taking into consideration

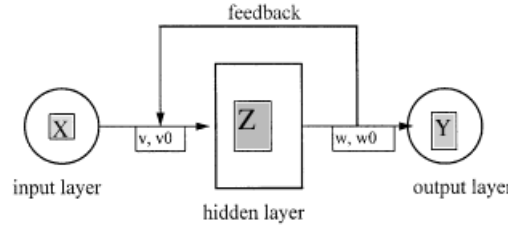

Figure 1. Typical architecture of recurrent neural network

a momentum parameter. Specifically, the update of weights and bias values is given by

$$\Delta V_{ij} = -\alpha \frac{\partial E}{\partial V_{ij}} + \mu \Delta V_{ij(\text{old})}$$

$$= \alpha \sum (T_k - Y_k) F'_2(Y_k) W_{jk} F'_1(Z_j) X_i + \mu \Delta V_{ij(\text{old})} \tag{4}$$

$$\Delta W_{jk} = -\alpha \frac{\partial E}{\partial W_{jk}} + \mu \Delta W_{jk(\text{old})}$$

$$= \alpha \sum (T_k - Y_k) Z_j F'_2(Y_k) + \mu \Delta W_{jk(\text{old})} \tag{5}$$

$$\Delta V_0 = \alpha \sum (T_k - Y_k) W_{jk} F'_1(Z_j) \tag{6}$$

$$\Delta W_0 = \alpha (T_k - Y_k) F'_2(Y_k) \tag{7}$$

where $E = 1/2 \sum_{k=1}^{n} (T_k - Y_k)^2$ is the sum of squared errors, α with value of (0, 1) is a learning rate, F'_1 and F'_2 are derivatives of the activation function of F_1 and F_2, respectively, and μ is a momentum parameter generally taking 0·5 to 1·0.

PROCEDURES OF MODELLING SOIL BEHAVIOUR WITH FEEDBACK CONNECTIONS

Modelling of soil behaviour with a neural network is a novel research area and it is expected[12] to be one of the leading modelling techniques in the 21st century for soil engineering mechanics. In applying RNN as a computational tool to the modelling of soil behaviour one has to consider the following aspects: (i) problem representation upon which the modelling speculation is made; (ii) design of RNN architecture, i.e. selecting the number of layers and nodes in each layer, as well as the interconnection scheme like forward, backward or recurrent propagation; (iii) determination of a specific optimization algorithm; (iv) initialization of training of RNN with input data upon which the relationship embedded in the data may be established and the weights between the neighbouring layers are obtained; (v) testing predictability of the trained network with testing data. These five aspects constitute a basic framework for modelling of soil behaviour presented in this paper.

Characteristics of soil behaviour and data base

Residual soil is a very heterogeneous soil due to its formation conditions. The shearing behaviour of the residual soil is much more complex than many common soils. In order to examine the ability of RNN modeling, a series of triaxial shearing tests were performed on a fine-grained residual volcanic soil. The soil was taken from a rainfall-induced landslide site on the island of Oahu, Hawaii. The properties of the soil vary greatly from point to point due to different environmental conditions. Standard sieve and hydrometer tests (ASTM D422) indicated that the soil contains about 10 per cent clay-size ($< 0{\cdot}002$ mm), 15 to 25 per cent silt-size (0·002 to 0·075 mm), and 65 to 75 per cent sand-size particles (0·075 to 4·75 mm). There are some gravel and cobble-size clasts of weathered basalt, most of which are vesicular and friable. The results of a series of Atterberg limit tests (ASTM D4318) show that the liquid limit of the soil ranges from 60 to 100 per cent with an average value of 78 per cent; the plastic limit is in a range of 53 to 79 per cent with an average value of 58 per cent; and, the plasticity index ranges from 9 to 35 with an average value of 19. According to standard test, the soil is classified (ASTM D2487) as SM soil.[19]

Triaxial shear test was conducted in a sequence of saturation, consolidation and shearing.[20] Saturation of a specimen was achieved by both a differential vacuum pressure and backpressure application. The vacuum process, with a maximum vacuum pressure -100 kPa, usually lasted for 1 h. The differential vacuum pressure between the inside and outside of the specimen was maintained less than 10 kPa in order to avoid overconsolidation of the specimen. Backpressure application was, after the vacuum process, proceeded by gradually increasing backpressure to about 200 to 250 kPa while maintaining an isotropic effective confining pressure as low as 10 kPa. B-values, defined as the coefficient of pore pressure, of 0·98 or above were achieved before the commencement of consolidation. Because of steepness of the slope site most specimens were consolidated in an anisotropic stress state and few were consolidated in an isotropic condition. Two types of shear tests were conducted to simulate the field shear stress paths. One type involved strain controlled undrained tests, while the other type involved stress controlled drained tests. The undrained tests were performed along two different stress paths: isotropic consolidation undrained (ICU) and anisotropic consolidation undrained (ACU) tests. The controlled strain rate was 0·1 per cent per minute and terminated at a strain value of 15 per cent. The ICU and the ACU tests are same as a conventional triaxial undrained test except that the consolidation stress ratio σ'_1/σ'_3 was 2·5 for all the ACU tests. For the drained tests, the specimens were first anisotropically consolidated to the field stress level, then the specimen was sheared by decreasing the effective confining pressure at a rate of 1 kPa/h while maintaining a constant shear stress, which is called a CSD test.[20–22] The CSD test was terminated when the specimen yielded or when the effective confining pressure reduced to zero. The CSD tests are considered as the best simulation of stress path for rainfall-induced landslides.[23,24] Table I gives a list of relative testing conditions and data

Table I. Data base used for training and testing in the RNN modelling

Test ID	Effective principal stress (kPa)		Initial PWP# u_0, kPa	Initial void ratio e_0
	$\sigma'_{3c}(\sigma'_{3f})$	$\sigma'_{1c}(\sigma'_{1f})$		
AC1*	16(18·7)	38(74·7)	200	3·14
AC2*	20(22·5)	50(77)	250	1·94
AC3	30(32)	75(133)	281	3·17
AC4	30(17·3)	75(65)	201	3·04
AC5	29(17·3)	73(71)	251	2·9
AC6*	45(25·6)	113(91)	200	2·29
IC1*	15·9(9·8)	17(67·6)	259	3·18
IC2*	45(29)	45(118)	251	3·45
IC3	31(18·5)	31(76)	229	3·83
IC4	30·5(15)	31(66)	210	3·18
CS1*	30(7·9)	75(44)	230	2·21
CS2*	24(4·4)	63(35·6)	305	2·48
CS3*	76(21·5)	190(96)	277	2·22
CS4	20(4·9)	50(25)	320	2·38
CS5	23(3·4)	56(34·6)	330	2·41
CS6	8(0·8)	36(21)	312	2·28
CS7	50(7·8)	125(68)	290	2·37

Note: 1 Data with * are the training data; rest are testing data.
2 Subscript o and f represent the onset and final state of the shearing test.
3 #PWP means pore water pressure.

base used for the RNN model. It was observed that the soil behaved differently with respect to the shearing response due to the significant variabilities of the soil structure and constituents.[20]

Some specimens tested at a low stress level dilated during the shearing process, while others tested at a high stress level experienced contraction. Consequently, the excess pore water pressure response was different for various specimens, i.e. a fairly high excess pore pressure was developed within the specimens subjected to contraction, while a low excess pore pressure was observed within the specimens which suffered dilation, as shown in the lower part of Figures 4–10. In CSD tests, the specimens underwent a sudden volume/and axial strain change when they approached yield.[20] Since the perimeter surface of the sample is rather rough and the tests were conducted at a very low confining pressure, membrane compliance and membrane resistance were corrected using a designed procedure.[25] Also, a cross-sectional area of the specimen was corrected using different models according to the failure mode of the soil specimen.[25,20]

Simulation of strain controlled tests

In a strain-controlled test, the stress–strain relationship of a soil can be expressed as

$$\{\Delta\sigma\} = [\mathbf{D}]\{\Delta\varepsilon\} \tag{8}$$

where $\{\Delta\sigma\}$ is the incremental stress vector; $[\mathbf{D}]$ is the coefficient matrix, usually called the constitutive matrix which is based on elastic modulus or elastic–plastic modulus of soil; $\{\Delta\varepsilon\}$ is the incremental strain vector that is known in advance.

The major objective in the ANN modelling is to search for something similar to the coefficient matrix $[\mathbf{D}]$ from which $\{\Delta\sigma\}$ can be found. According to the procedure described earlier, the following choices are made regarding the design of the RNN model for strain-controlled shear tests:

(1) *Input variables and output results:* An appropriate selection of the input and output is important for a successful simulation using the RNN model. In strain-controlled shearing tests the axial strain and strain rate as independent variables are given to find out response of stress which is a dependent variable. So, the current axial strain $\varepsilon_{1,i}$ and increment of the strain $\Delta\varepsilon_{1,i}$ should be the input variables, while the stress responses at $i+1$ step, i.e. deviator stress $\mathrm{dev}\,\sigma_{i+1}$ and pore water pressure u_{i+1}, are considered as outputs. It is well understood from the literature[2,20] that the stress–strain behaviour of a soil is greatly influenced by such important factors as stress history, consolidation condition and void ratio. The change of the void ratio in the undrained tests is a result of membrane compliance occurred when effective confining pressure decreases.[19] Therefore, the effective confining pressure σ'_{3i}, previous deviator stress $\mathrm{dev}\,\sigma_i$, pore water pressure u_i and void ratio e_i are considered as inputs, too. It should be pointed out that the values of $\mathrm{dev}\,\sigma_i$ and u_i are nothing but the outputs from the network's forward computation of the last epoch, or $i-1$ step, while the value of σ'_{3i} is the difference between the total confining pressure σ_3 which is known ahead and pore water pressure u_i.

(2) *Architecture of the model:* After trying different number of hidden layers, one hidden layer with connections to both input layer and output layer is used in the RNN model employed here. One hidden layer is actually considered as being able to model any non-linear work,[13,14] although sometimes multiple hidden layers may efficiently deal with complex problems.[15] The number of nodes in the hidden layer is determined by a trial-and-error method. In the preliminary study, a network with different nodes ranging from 4 to 30 in the hidden layer was trained for the same number of epochs, and the sum of squared errors (SSE) of the training sets was recorded. It

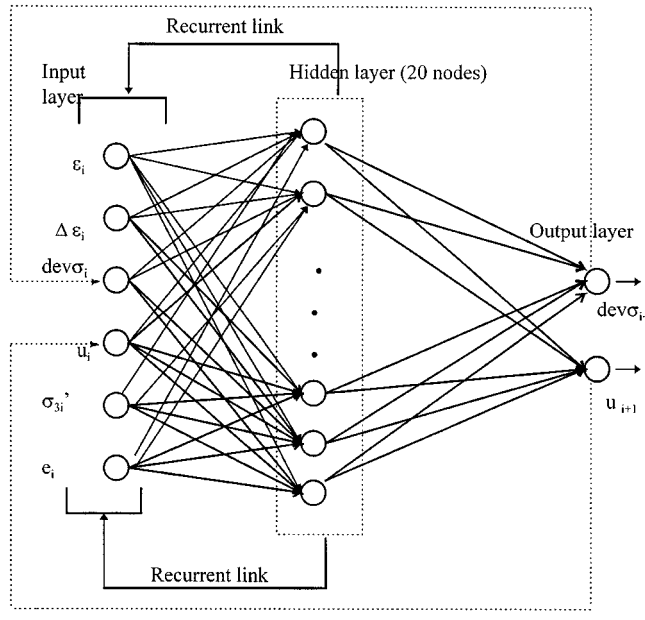

Figure 2. Architecture of $6 \times 20 \times 2$ recurrent neural network for strain-controlled ACU and ICU

was found that the value of SSE reached minimum when the number of nodes equaled 20. So a $6 \times 20 \times 2$ network is set up as shown in Figure 2. It is noted that once the initiation of training process commences the original network becomes a $26 \times 20 \times 2$ network, since the 20 outcomes from the hidden layer are transmitted back to the input layer and work as new input again.

(3) *Learning process:* Learning algorithm is set as folows:

Step 1: For each input vectors $\mathbf{s}_i$ ($i = 1, 2, 3, \ldots, n$) perform step 2 to step 9;
Step 2: set $\mathbf{x} = \mathbf{s}_i$;
Step 3: if $m = 1$, set the initial weights and biases v_{ij}, w_{jk}, v_0, w_0 randomly;
and go to step 5;
otherwise go to step 4;
Step 4: load previously achieved weights and biases and set them as initial weights and biases;
Step 5: if stop condition is false perform step 6 to step 9;
Step 6: calculate Z_j, and Y_k using equations 2 and 3;
Step 7: calculate $E = 1/2 * \sum_{k=1}^{n} (T_k - Y_k)^2$;
Step 8: update weights and biases using equations (4)–(7);
Step 9: test if stopping conditions have been satisfied.

In the RNN model, the hyperbolic tangent function ($F_1(x) = (e^x - e^{-x})/(e^x + e^{-x})$) is generally used as an activation function from the input layer to the hidden layer while in the connection between the hidden layer and the output layer a linear transform function ($F_2(x) = a + bx$) is adopted.

(4) *Training process:* The training process is initialized by inputting a set of 'comprehensive' data to the network. The so-called 'comprehensive' data imply that the data are most representative and contain all the necessary information for the given problem. A network trained with the

comprehensive data is expected to have a strong predictability. It is necessary, from our experience, to normalize every set of data with respect to its maximum and minimum values before initiating the training process. After normalization, each set of data value is presented within a range of (0, 1), with their maximum and minimum values represented by 1 and 0, respectively. This preprocessing of data guarantees that the network operates in a more efficient and more reliable manner. The flexibility of the network itself ensures that the network can be trained ceaselessly until the comprehensive data are included in the training data base. As indicated in Table I the test data sets numbered as AC1, AC6, IC1, IC2 were used as the training data since they contain possible range of the testing stresses.

It is worth mentioning that the training of strain-controlled test data with the RNN may be different from conducting a laboratory experiment, i.e. the increment of strain is unnecessary to be a constant for a given data set. In the laboratory, the data acquisition system recorded experimental data automatically at a rate of 10 records per minute. There are about 9000 sets of data in one laboratory test. To save computer memory space and operation time, the original data were reduced and shifted substantially. The data set to be used in the RNN model only contains about 40 to 60 records. Therefore, the strain increments in one set of test data range from about 0·0001 to 0·5 per cent. It is observed that these differences actually have no adverse effects on the training process, but makes the network more applicable in the situation where a wide range of strain rates might exist. The training process was performed with Matlab on a PC/Gateway 2000 (Pentium 586) computer. In order to enhance flexibility of the network, the training process of the network was also designed as a dynamic system that can make use of previous knowledge in the case of training new data and when more epochs of training are required. It was found that after 10 000 epochs the sum squared error reached 0·05, which took about 180 min of CPU time, after which the sum squared error almost maintained a constant.

(5) *Testing of networks:* After training, the network produces 20×26 weights and 20 bias values connecting input layer and hidden layer, and 2×20 weights and 2 bias values connecting hidden layer and output layer. Due to limitation of the space those weight and bias values are not presented in the paper, but they are available upon request. With these weights and biases the network was tested with both trained and untrained data to examine its simulation capability and accuracy.

Simulation/prediction results. Figures 3–6 show the RNN simulation of the ACU and ICU test results with the trained data. There are two kinds of results shown in these figures. One set of curves represent shear stress versus axial strain values. The other set shows the relationship between the pore water pressure and the axial strain. From Figure 3, one can see that there is an apparent peak shear stress beyond which the shear stress decreases with the increasing axial strain. When using the conventional mathematical model the negative modulus will appear in the strain softening region[1] that tends to increase the mathematical modelling effort significantly. It should also be pointed out that the ACU shearing tests are initialized at a non-zero shear stress that is difficult to be modelled by many mathematical models.[1,2] It is realized that the simulation of pore water pressure u is difficult since the excess pore pressure developed varies significantly for different specimens. Some discrepancy between the simulated pore pressure and experimental pore pressure is observed at the initial excess pore pressure developing stage after which the simulation is fairly satisfactory.

Figures 7–10 demonstrate the predictability of the RNN model with respect to laboratory experimental data. Although the RNN model did not gain anything from these untrained data,

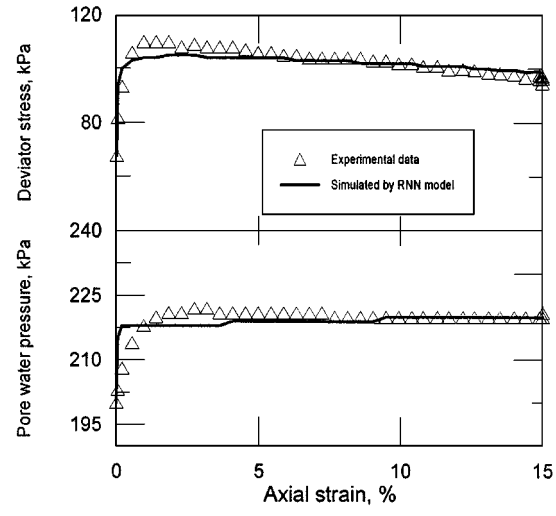

Figure 3. RNN simulation of ACU test results with trained data: AC6

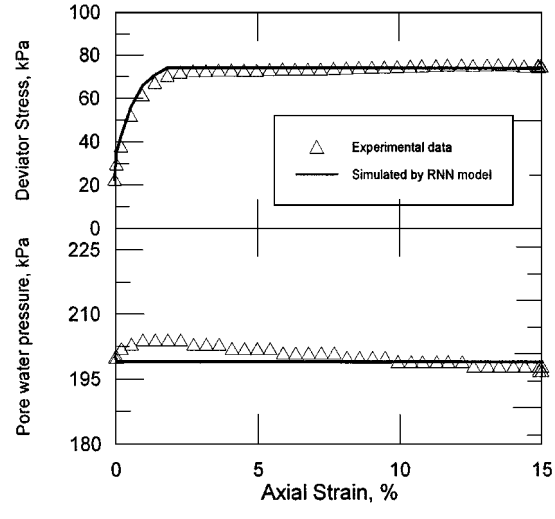

Figure 4. RNN simulation of ACU test results with trained data: AC1

the RNN prediction of stress–strain relation is very encouraging based on the information learnt from the training data. Both the zero and non-zero initial shear stress conditions are captured well by the RNN model, and the different shear behaviour including dilation and compaction are represented consistently by the RNN model. The prediction of pore water pressure shows similar trend as did in simulation cases, i.e. at initial stage of excess pore pressure development there is some discrepancy between the predicted value and experimental data; at later course of shearing where excess pore pressure has fully developed the prediction is fairly satisfactory.

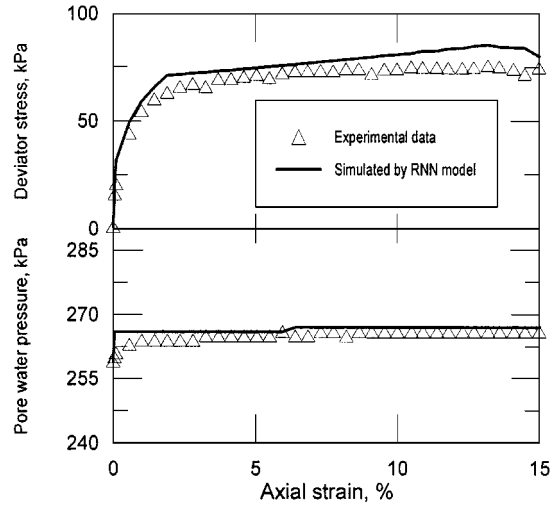

Figure 5. RNN simulation of ICU test results with trained data: IC1

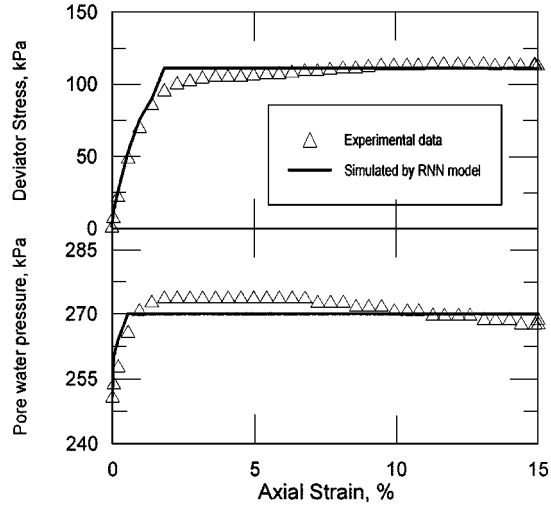

Figure 6. RNN simulation of ICU test results with trained data: IC2

From the preceding discussion, it is evident that with the RNN modelling one does not need to find a series of material parameters describing mathematical equations associated with a constitutive model. This is one of the important advantages of the RNN model over a traditional constitutive model, since the computation of material parameters is usually a very tedious and difficult process, and therefore prone to error.

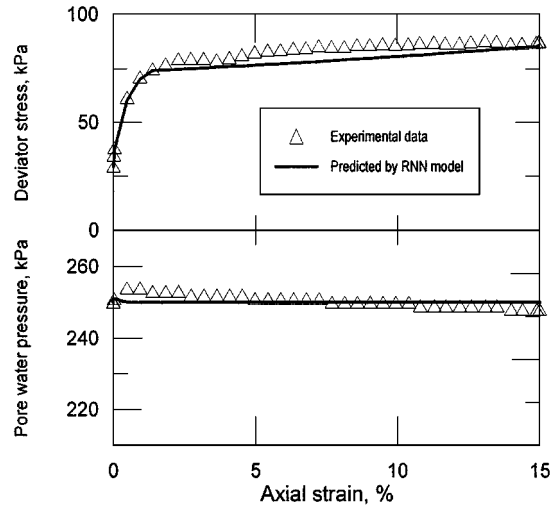

Figure 7. RNN prediction of ACU test results with untrained data: AC2

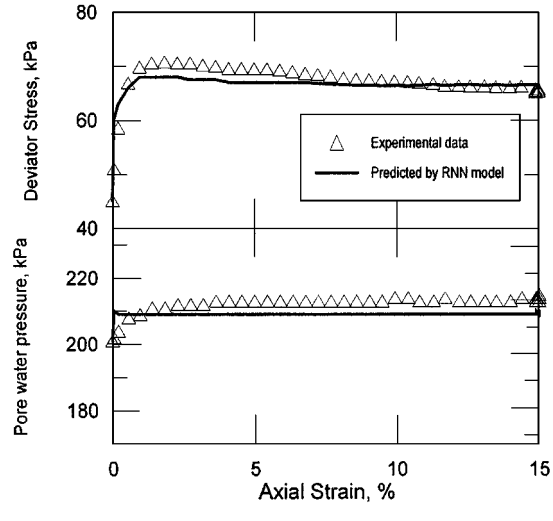

Figure 8. RNN prediction of ACU test results with untrained data: AC4

Simulation of the stress-controlled tests

In the stress-controlled tests used in this paper the soil was subjected to shearing under a constant shear stress while gradually decreasing the effective confining stress, which is called CSD test. This shearing condition represents mostly the field failure stress paths under a rainfall-induced landslide.[20,21] The modelling of a stress-controlled test follows the procedures presented

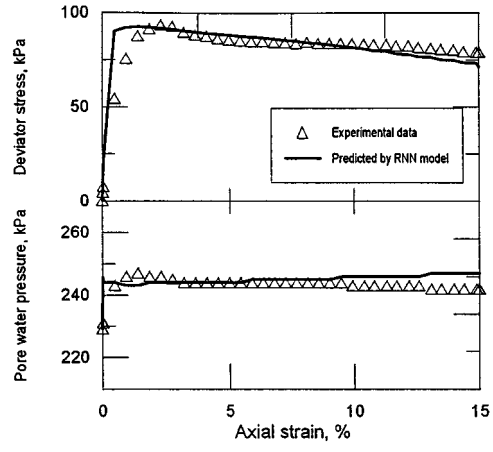

Figure 9. RNN prediction of ICU test results with untrained data: IC3

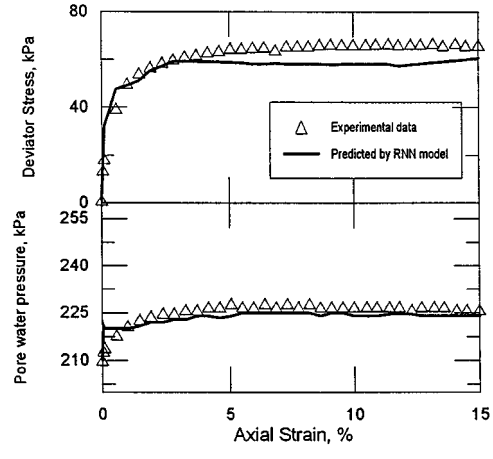

Figure 10. RNN prediction of ICU test results with untrained data: IC4

before except the choice of input and output variables in the network. Since the effective stresses are specified in the experiment, the current effective confining pressure σ'_{3i}, effective principal stress σ'_{1i} and their increments $\Delta\sigma'_{3i}$, $\Delta\sigma'_{1i}$ are used as the input variables. During the CSD test, the axial and volumetric strain values are monitored to see whether the soil specimen has failed. So, the outputs for such a test are the axial strain $\varepsilon_{1,i+1}$ and volumetric strains $\varepsilon_{v,i+1}$, which are corresponding to the inputs of current stress and stress increment. Also, considered in the input are void ratio, previous axial strain $\varepsilon_{1,i}$ and volume strain $\varepsilon_{v,i}$ which are the outputs of the network's computation at $i-1$ epoch. Using a trial-and-error method, one hidden layer with 35 nodes was chosen as an intermediate layer between the input and output layers. The architecture

of the RNN model with $7 \times 35 \times 2$ structure is shown in Figure 11. Also, same as stated before, once initiated the original network becomes a network with $42 \times 35 \times 2$ nodes in its structure. Consequently, there are 42×35 weights and 35 bias values in connecting input layer and hidden layer, 35×2 weights and 2 bias values between hidden layer and output layer.

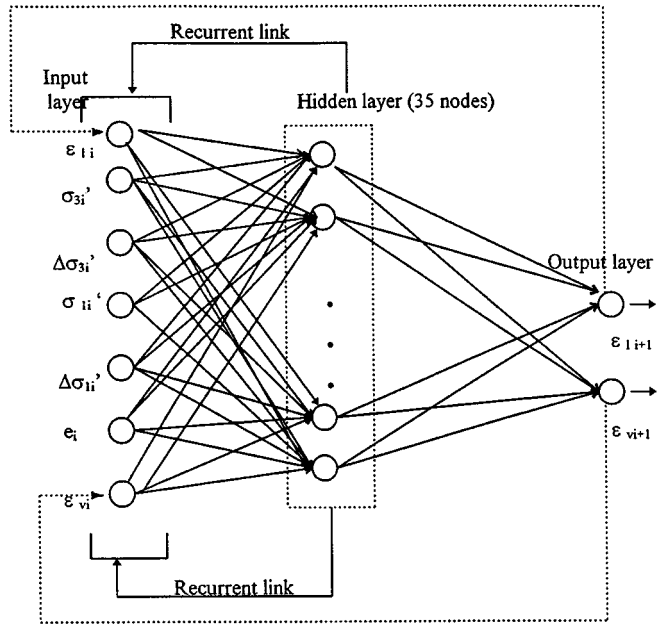

Figure 11. Architecture of $7 \times 35 \times 2$ recurrent neural network for stress-controlled CSD test

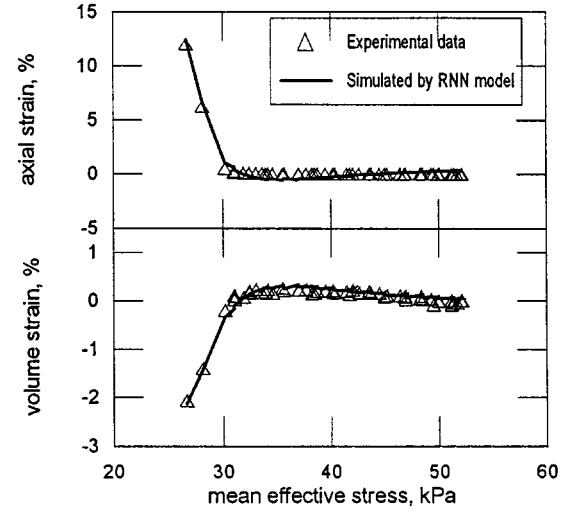

Figure 12. RNN simulation of the CSD test results with trained data: CS1

Similar to the strain increments described in modelling of the strain-controlled tests, the stress increments prescribed in the RNN model are also not constants. In some steps, the increment might be zero, while in certain steps the increment might be equal to or greater than 1kPa, due to sifting and reduction of the data. These reductions were observed to be not harmful to the network but save computer time significantly.

Figures 12 and 13 show the simulation results of the RNN model for the two tests that are used in training the model. Figures 14 and 15 demonstrate the predictability of the RNN model for the

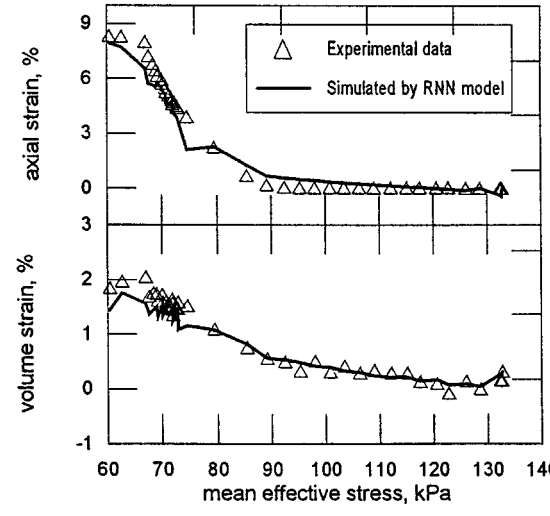

Figure 13. RNN simulation of the CSD test results with trained data: CS3

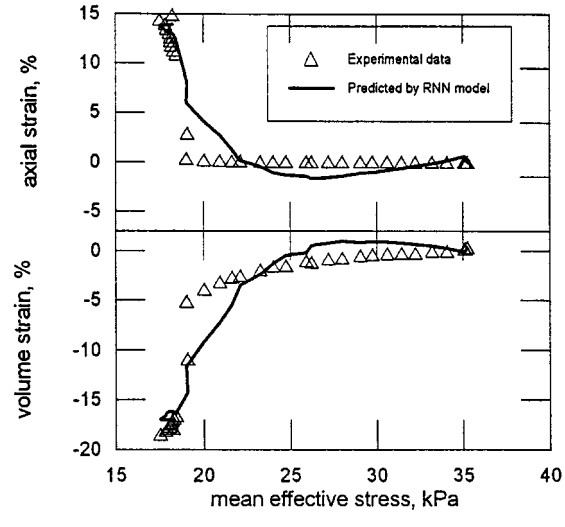

Figure 14. RNN prediction of the CSD test results with untrained data: CS4

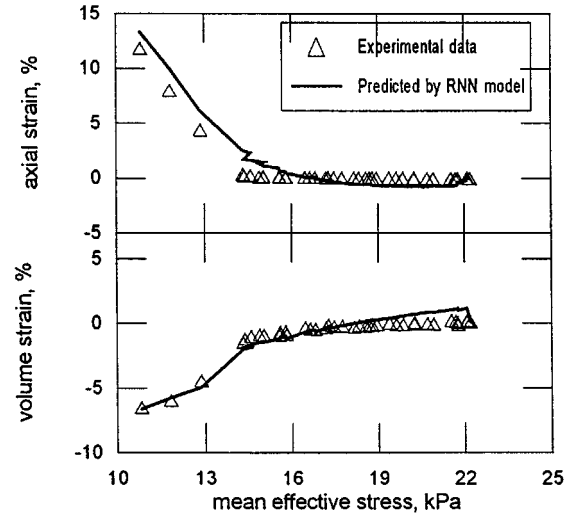

Figure 15. RNN prediction of the CSD test results with untrained data: CS6

test data not used in the training process. It can be seen from these figures that both simulation and prediction results are in good agreement with the measured values. It should be noticed that the failure of the soil specimens in the CSD test occurred rather abruptly. Specifically, the strain values at the commencement of failure were much higher than those prior to the failure where the variations in strain were actually negligible. This special behaviour is difficult to model by a conventional mathematical constitutive model, and even by some fairly complex constitutive models.[2,26,6,7]

DISCUSSIONS

Research work on residual soils has achieved much less than that on common soils in both laboratory experiments and numerical models. The significant variability in constituents and structures of the residual soils has brought about unusual behaviour when subject to shear stress. The dilative response can be found in the specimens with low density and tested at high-stress level, while contractive behaviour is observed in the specimens with high density and tested at low-stress level. The neural network provides an effective alternative for modelling shearing behaviour of the residual soils. The efficiency and adaptability of the RNN model is demonstrated by successful simulation/and prediction of various behaviour of the residual soil used in this study. As compared with the traditional constitutive models, the RNN model has same following salient features as other neural networks:

(1) The model is essentially based on experimental data only. No assumptions are made, which allows the model to become more objective rather than subjective. In other words, the RNN model is not to be influenced by the shape of stress–strain curves. This feature is of particular significance in dealing with soil constitutive behaviour. Since the properties of soil varies from place to place, the successful application of a constitutive model in one case contributes no direct benefits to another case. However, the results in terms of weights and bias values obtained from

the RNN model can be easily shared by others, such as using these weights and bias values as either initial values to train their own experimental data or real connections to predict corresponding outputs, if any. With continuously updating the weights and bias values by training new set of data, the RNN model is able to store more comprehensive information associated with soil shear behaviour. Once the real comprehensive data are trained, the RNN model will become more effective and robust.

(2) The RNN model is set-up without any calculation of parameters required by a mathematical constitutive model. These calculations result in one of the error sources in the application of most constitutive models. Meanwhile, the equations required in the RNN model are much less than those used in a conventional constitutive model and the implementation of the RNN model only involves a series of iteration calculations performed by a computer which is easily available currently. Therefore, the RNN model is a simple and effective modelling approach, if appropriate experimental data are available.

In addition, the RNN model developed in this paper shows more flexible and less restriction regarding the data input, as compared with other neural network models. In the sequential and regular neural network, Penumadu[10] reported that a fixed value of axial strain rate is required for prediction of the soil behaviour, which limits application of their results.[9] It appears that less experimental data are required in training the RNN model developed in this paper and the neural connections thus obtained are still effective and robust, as illustrated by the capturing of special shear behaviour of the soil specimens. Although the choice of input and output variables is important in the design of the network, a highly efficient computer-based computation enables an easy alternation of the variables. So, the RNN model is also a time-saving model.

CONCLUSIONS

Application of the neural network to the modelling of soil behaviour is a novel research area. The successful modelling of the shear behaviour of a residual volcanic soil described in this paper demonstrates the capabilities of the RNN model. Although the soil exhibited both dilative and contractive behaviour during shearing, the RNN model captured these variabilities accurately and efficiently. Both hardening and softening properties are represented by the RNN model. The pore water pressure response is simulated simultaneously while modelling the stress–strain behaviour. The substantial variations in axial and volumetric strains which occurred in the CSD tests are characterized by the RNN model. The design of the architecture of the RNN model varies with the characteristics of a problem. In this study, one hidden layer with 20 and 35 nodes was found to be suitable for the modelling of the strain-controlled undrained tests and the stress-controlled drained tests, respectively. The proposed RNN model appears to be more flexible regarding the input requirements than other neural network models.

ACKNOWLEDGEMENTS

The experimental study reported here was supported by the National Science Foundation Grant No. BCS92-11927. The research work on the RNN modeling was supported in part by the Oklahoma Department of Transportation and the School of Civil Engineering and Environmental Science at the University of Oklahoma. These supports are gratefully acknowledged by the authors.

REFERENCES

1. J. M. Duncan and C. Y. Chang, 'Nonlinear analysis of stress and strain in soils', *J. Soil Mech. Foundations Div. ASCE*, **96** (SM5), 1629–1653 (1970).
2. C. S. Desai, 'Modeling and testing: implementation of numerical models and their application in practice', Desai and Gioda, (eds.) *Num. Meth. and Const. Mod. in Geomech*, Springer, Wien, New York, 1990, pp. 1–28.
3. R. J. Borja, 'Generalized creep and stress relaxation model for clays', *J. Geotech. Engrg. ASCE*, **118** (11), 1765–1786 (1992).
4. A. J. Whittle, D. J. DeGroot, C. C. Ladd and T. H. Seah, 'Model prediction of anisotropic behavior of boston blue clay', *J. Geotech. Engng. Div. ASCE*, **1** (1), 199–224 (1994).
5. C. S. Desai, G. Frantziskonis and S. Somasundaram, 'Constitutive modeling for geological materials', *Proc. 5th Conf. On Numer. Meth. In Geomech*., Nagya, Japan, 1985, pp. 19–34.
6. M. O. Faruque, 'A third invariant dependent cap model for geological materials', *J. Soils Found. ASCE*, **27,** 12–20 (1987).
7. M. Zaman, M. O. Faruque and A. Abdulraheem, 'Three invariant dependent characteristic state model for cohesionless soil', *Int. J. Numer. Anal. Meth. Geomech*., 1997 (in review).
8. G. W. Ellis, C. Yao, R. Zhao and D. Penumadu, 'Stress–strain modelling of sands using artificial neural networks', *J. Geotech. Engng. Div. ASCE*, **121** (5), 429–435 (1995).
9. Y. M. Najjar and I. A. Basheer, 'Discussion of stress–strain modelling of sands using artificial neural networks', *J. Geotech. Engrg. ASCE*, **122** (11), 949–950 (1996).
10. R. Penumadu, 'Discussion of stress–strain modeling of sands using artificial neural networks', *J. Geotech. Engrg. ASCE*, **122** (11) , 950–952 (1996).
11. B. Widrow and M. A. Lehr, '30 years of adaptive neural networks: perceptron madaline and backpropagation', *Proc. IEEE*., **78** (9), 1415–1442 (1990).
12. J. Ghaboussi, 'Neural-biological computational models with learning capabilities and their applications in geomechanical medeling', *Proc. of Recent Accomplishments and Future Trends in Geomechanics in the 21st Century*, U.S. Canada Workshop. Edited by Zaman, Desai and Selvadurai, Norman, Oklahoma, 1992, pp. 131–134.
13. C. L. Giles, G. M. Kuhn and R. J. Williams, 'Dynamic recurrent neural networks: theory and applications', *IEEE Trans. Neural Network*, **5** (2), 153–160 (1994).
14. J. L. Elman, 'Finding structure in time', *Cognitive Sci*., **14,** 179–211 (1990).
15. A. G. Parlos, K. T. Chong and A. F. Atiya, 'Application of the recurrent multilayer perception in modeling complex process dynamics', *IEEE Trans. Neural Network*, **5** (2), 255–285 (1994).
16. J. T. Connor, R. D. Martin and L. E. Atlas, 'Recurrent neural networks and robust time series prediction', *IEEE Trans. Neural Network*, **5** (2), 240–254 (1994).
17. D. Rumelhart, G. E. Hinton and R. J. Williams, 'Learning internal representations by error propagation', Rumelhart and McClelland (eds.), *Parallel Data Processing*, M.I.T. Press, Cambridge, 1986, pp. 318–362.
18. T. P. Vogl, J. K. Mangis, A. K. Rigler, W. T. Zink and D. L. Alkon, 'Accelerating the convergence of the back propagation method', *Biol. Cybernet*. **59,** 257–263 (1988).
19. J. H. Zhu, 'Shear strength and soil behavior on a residual soil slope', *Civil Engineering Master's Thesis*, University of Hawaii-Manoa, Honolulu, Hawaii, 1995.
20. J. H. Zhu and S. A. Anderson, 'Determination of shear strength for Hawaiian residual soil subjected to rainfall-induced landslide', *Geotechnique*, **48** (1), (1998) (in press).
21. S. A. Anderson and N. Sitar, 'Analysis of rainfall-induced debris flows', *J. Geotech. Engrg. ASCE*, **121** (7), 544–552 (1995).
22. S. A. Anderson and J. H. Zhu, 'Assessing the stability of a tropical residual soil slope', *Proc. 7th Int. Symp. on Landslides*, Norway, 1996.
23. E. W. Brand, 'Some thoughts on rain-induced slope failures', *Proc. 10th Int. Conf. On Soil Mech. and Found. Engrg*., Vol. 3, Stockholm, Sweden, pp. 373–376.
24. N. Sitar, S. A. Anderson and K. A. Johnson, 'Conditions for initiation of rainfall-induced Debris flows', *Proc. of the Stability and Performance of Slope and Embankments—II*, Vol. 1, ASCE, New York, 1992, pp. 834–849.
25. J. H. Zhu and S. A. Anderson, 'Corrections for triaxial tests on undisturbed soils', *J. Testing Evaluation ASTM*, (5), 1998 (in press).
26. C. S. Desai, 'A consistent finite element technique for work-softening behavior', *Proc. Int. Conf. Comput. Methods Nonlinear Mech*., Austin, TX., 1974, pp. 969–978.
27. R. J. Borja and A. P. Amies, 'Multiaxial cyclic plasticity model for clays', *J. Geotech. Engrg. ASCE*, **120** (6), 1051–1992 (1994).
28. C. S. Desai and G. W. Watagala, 'Constitutive model for cyclic behavior of clays', *J. Geotech. Engng. Div. ASCE*, **119** (4), 714–729 (1993).
29. K. Hoeg, 'Finite element analysis of strain-softening clay', *J. Soil Mech. Found. Div. ASCE*, **98** (SM1), 43–58 (1972).
30. H. S. Hsieh, E. Kavazanjian Jr. and R. I. Borja, 'Double-yield surface cam-clay plasticity model. I: theory', *J. Geotech. Engrg. ASCE*, **116** (9), 1381–1401 (1990).
31. R. L. Kondner, 'Hyperbolic stress–strain response: cohesive soils', *J. Soil Mech. Found. Div. ASCE*, **89** (SM1), 115–143 (1963).

